JOURNAL OF MATERIALS SCIENCE 9 (1974) 1839–1846

# Microhardness investigations on manganese aluminate spinels

E. H. L. J. DEKKER, G. D. RIECK
*Laboratory of Physical Chemistry, Eindhoven University of Technology, Eindhoven, Netherlands*

Vickers microhardness measurements were carried out on single-crystalline manganese aluminates having compositions ranging from $Mn_{1.83}Al_{1.17}O_4$ to $Mn_{0.91}Al_{2.06}\square_{0.03}O_4$. Hardness increases with increasing alumina content, but the hyperstoichiometric composition shows a decline of hardness probably due to structural vacancies. In $Mn_{1.83}Al_{1.17}O_4$ the crack pattern round indentations is independent of relative indenter orientation and can be accounted for by the presence of a {110} glide system. Apparent hardness anisotropy is related to the position of these glide planes in the surface. In all other harder specimens of this series, other glide systems also become operative during indentation. The occurrence of a pre-precipitation phase after the annealing of specimens is revealed by an increase in hardness, followed by a decline which is due to over-ageing.

## 1. Introduction

Although Bückle [1, 2] has pointed to the possibility of investigating various material properties by means of microhardness measurements, he has imposed some restrictions on the interpretation of hardness anisotropy data. Indenting causes a general piling-up of matter with an additional rim round the indentation, which in metals is responsible for variations in observed diagonal lengths and shape of indentations with different relative indenter orientations. Therefore, the hardness measured on a certain crystallographic plane will be influenced by the particular glide systems operating in plastic deformation round the indentation. This influence has also been demonstrated on lead sulphide and some halogenides [3, 4], and a model has been proposed by Boyarskaya based on downward movement followed by an upward one of displaced matter along the glide planes [5]. On oxide materials, hardness anisotropy has been mostly determined using a Knoop indenter and shown to be dependent on the relative orientation of the long axis of the diamond and the specimen surface [6, 7].

In the present work, Vickers microhardness data are given of spinel-type manganese aluminates of varying composition, and some anisotropy effects discussed in the light of the known glide systems in spinels. In addition, the early stage of precipitation is investigated on Mn–Al spinels supersaturated with $Al_2O_3$. Available literature data on the influence of precipitation on hardness of spinels refer mostly to the $MgAl_2O_4$–$Al_2O_3$ system, in which a pre-precipitation phase is transformed into the intermediate $\phi$–$MgAl_{26}O_{40}$ and the stable $\alpha$–$Al_2O_3$ (corundum) [8]. Though strength of Mg–Al spinels (determined by fracture-load measurements) is at its maximum in the pre-precipitation stage [9], maximum hardness occurs only after the $\phi$-phase precipitation becomes observable (whether measured by determination of corrosion hardness [10], Knoop low-load hardness [11], Knoop microhardness [12], or Vickers microhardness [13, 14]). In the $MgAl_2O_4$–$Cr_2O_3$ system the elastic strain energy is at its maximum during $\phi$-phase segregation [15]. In the $Mn_3O_4$–$Al_2O_3$ system corundum precipitation is preceded by the occurrence of the intermediate $\gamma$-$(Mn,Al)_2O_3$ phase, which is different from the $\phi$ phase mentioned [16]. It seems of interest to compare the hardness behaviour during segregation in Mn–Al spinels with that in Mg–Al spinels.

## 2. Experimental procedure

Single-crystalline manganese aluminates were grown from the sintered oxides in an arc-image radiation furnace using a floating-zone technique, as reported earlier [17]. Cleft or sawn slices were embedded in resin, ground with SiC

paper down to 600 grit and consecutively polished during 30 min with diamond pastes of 6 and 1 μm grain size, respectively. As additional polishing during 2 h did not significantly lower the hardness values, surface hardening was negligible. Orientations of the slices were checked by means of X-ray Laue diagrams.

Microhardness indentations were made with a Vickers diamond, using the Leitz "Durimet" hardness tester. The diamond was run down at a loading rate of about 100 μm $sec^{-1}$, which rate causes observed hardness numbers to be 3.3% too low [2]. Loads of 25 to 500 gf were applied during about 5 sec. This duration, however, proved not to be critical as an extension up to 15 sec did not cause any significant change in hardness number. The term "microhardness testing" is used in this work, in accordance with Bückle [1, 2], with respect to indentation diagonal length rather than to applied load.

For each determination a series of 10 to 20 indentations was made. Diagonal lengths were measured using a separate microscope with calibrated ocular at magnification × 1000. From the mean of each pair of diagonals of one indentation, the average and standard deviation of the whole series was calculated. The 95% confidence interval was determined using Student's *t*-distribution and is given with the results in tables and figures. However, the actual, absolute values of hardness might lie outside this interval on account of individual bias in measuring the indentations. Another possible cause of systematic errors, raising the apparent hardness, is to be found in the strains of the specimens due to thermal gradients during crystal growth. This effect was eliminated by annealing $Mn_{1.83}Al_{1.17}O_4$ specimens at 1410°C for 3 days. Specimens with higher alumina content were not annealed because precipitation might occur, and so they may show a hardness that is too high. A third cause of systematic errors, lowering the apparent hardness by 3.3%, constitutes the high loading rate mentioned above.

## 3. Results and discussion

### 3.1. Influence of orientation

For this investigation specimens of the composition $Mn_{1.83}Al_{1.17}O_4$ were mainly used. Even under the smallest load (25 gf) cracks occurred round the indentations. As stated earlier on Mg–Al spinel, among other minerals [6], these cracks and observed lengths of indentation diagonals are fairly consistent for a given crystallographic plane and orientation. On a (001) plane the main cracks always lie in ⟨110⟩ directions regardless of relative orientation of the indenter (Fig. 1a and b). Piling-up of displaced matter is also similar for indentation diagonals lying parallel to ⟨110⟩ or ⟨100⟩, and reaches a

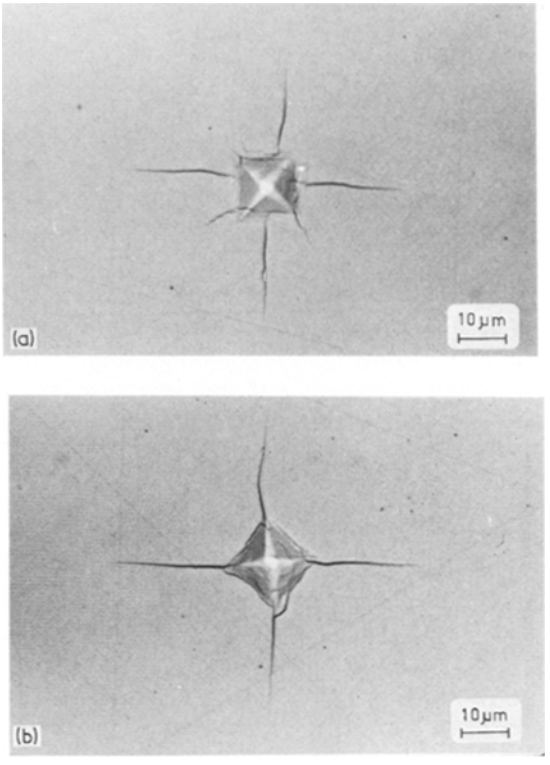


*Figure 1* (a) $Mn_{1.83}Al_{1.17}O_4$, (001) plane, indentation diagonals parallel to ⟨100⟩, 200 gf load, polarized light. (b) Indentation diagonals parallel to ⟨110⟩.

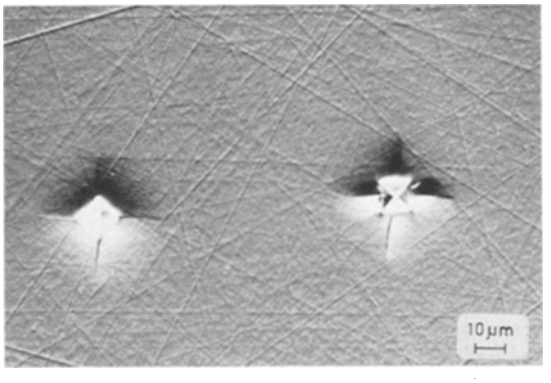


*Figure 2* Interference contrast showing height differences on $Mn_{1.83}Al_{1.17}O_4$, (001) plane, indentation diagonals parallel to ⟨110⟩ (left) and ⟨100⟩ (right), 100 gf load.

TABLE I Influence of relative orientation of indenter on the length of indentation diagonals on (001) plane of $Mn_{1.83}Al_{1.17}O_4$

| load (gf) | Indentation diagonals along: ⟨110⟩ | | ⟨100⟩ | |
|---|---|---|---|---|
| | Diagonal length (μm) | Hardness (kgf mm$^{-2}$) | Diagonal length (μm) | Hardness (kgf mm$^{-2}$) |
| 200 | 18.4 ± 0.1 | 1090 ± 15 | 18.1 ± 0.3 | 1135 ± 40 |
| 100 | 12.63 ± 0.12 | 1165 ± 20 | 12.35 ± 0.16 | 1215 ± 35 |
| 50 | 8.67 ± 0.09 | 1235 ± 25 | 8.64 ± 0.12 | 1240 ± 35 |
| 25 | 5.92 ± 0.06 | 1320 ± 20 | 5.85 ± 0.06 | 1355 ± 25 |

maximum at the cracks (Fig. 2). From this it may be expected that the diagonals will be shorter when lying along ⟨100⟩ than along ⟨110⟩, because the diagonal ends are situated in the valleys in the former case, but on the hills in the latter case. This is confirmed by the trend of Table I, though the effect is rather small.

The ⟨110⟩ directions of the cracks can be accounted for by assuming those {110} planes which intersect the (001) surface at 45° to be the effective glide planes. In the (001) plane the ⟨110⟩ directions constitute the projections of the boundaries between each two glide planes and the cracks result from the divergency of matter (or piling-up of dislocations on the intersection of two glide planes, as demonstrated on MgO [18]). Once the cracks are formed, glide will proceed less hampered in their vicinity, resulting in a somewhat higher piling-up at the cracks. This picture is consistent with the one proposed by Boyarskaya for scratch hardness anisotropy [5], in which the hill of pressed-out matter is larger near the intersection of two glide systems compared to the one of a single glide system. Glide systems of Mg–Al spinels at high temperature are known to be mainly of the $\{110\}\langle 1\bar{1}0\rangle$ and $\{111\}\langle 1\bar{1}0\rangle$ types [19-22]. These also occur in Mn–Zn ferrites at room temperature [7], whereas in $Fe_3O_4$ {100} and {111} glide planes occur [23].

Hardness variations of different crystallographic planes, represented in Table II, are largest when measured under low loads. Probably plastic deformation, though determining the initial crack formation, has relatively less importance at higher loads, where fracture along fracture planes might occur. Adsorption of water from the air might also play a part in case of lower loads [24, 25]. Consideration of possible glide planes should not only include angles of intersection with the investigated surface planes, but also the distribution of glide planes round the indentation, because at least one glide direction on each side of the indentation is necessary. Concerning the glide plane itself regarded as the surface plane, it provides at least two opposite glide directions and should, therefore, likewise be considered in a comparative study of the surface planes.

By comparison with Table III it can be seen that hardness of different planes increases with increasing angles of intersection of a set of {110} planes with those planes, whereas no such relation exists for the intersection of {111} or {100} planes with the investigated surface planes. Extending the model proposed by Boyarskaya and Grabko [5], it can be presumed that downward displacement of matter is less hindered by the associated upward movement when the angle between the two directions along which these glide movements occur is larger. This strengthens the conclusion that {110} glide planes are operative.

On specimens with higher alumina content and also at the outer surface of an $Mn_{1.83}Al_{1.17}O_4$ specimen, crack patterns become more complicated with indentation diagonals lying along ⟨100⟩ on a (001) surface (Fig. 3a), though remaining simple in the ⟨110⟩ case (Fig. 3b). On these harder materials the four-fold indenter symmetry probably induces other glide planes to be effective when {110} planes are in an inconvenient position. If the load is too high, deformation is too severe and near the indentations displaced matter chips off (Fig. 4), as observed frequently on minerals [4, 26]. This does not alter the size of the indentations if the diagonal ends can still be observed.

### 3.2. Compositional dependence

The relationship of hardness with composition of as-grown crystals is shown in Fig. 5. The steep

TABLE II Microhardness on different planes of $Mn_{1.83}Al_{1.17}O_4$

| Plane | Indentation diagonals | Microhardness (kgf mm$^{-2}$), using: 200 gf load | 50 gf load |
|---|---|---|---|
| (110) | [1$\bar{1}$0] and [001] | 1105 ± 15 | 1130 ± 25 |
| (111) | [1$\bar{1}$0] and [11$\bar{2}$] | 1105 ± 35 | 1200 ± 30 |
| (001) | [1$\bar{1}$0] and [110] | 1090 ± 15 | 1235 ± 25 |
| (103) | ~[3$\bar{3}$1] and [33$\bar{1}$] | 1145 ± 15 | 1335 ± 15 |
| (103) | [30$\bar{1}$] and [010] | 1160 ± 15 | 1320 ± 30 |

TABLE III Interplanar angles with {110}, {100} and {111} planes in the cubic system

| Plane | Interplanar angles (°) with: | | | | | |
|---|---|---|---|---|---|---|
| | {110} | Number | {100} | Number | {111} | Number |
| (110) | 0 | 1 | 45 | 2 | 35.3 | 2 |
| | 60 | 4 | 90 | 2 | 90 | 2 |
| | 90 | 1 | | | | |
| (111) | 35.3 | 3 | 54.7 | 3 | 0 | 1 |
| | 90 | 3 | | | 70.5 | 3 |
| (100) | 45 | 4 | 0 | 1 | 54.7 | 4 |
| | 90 | 2 | 90 | 2 | | |
| (103) | 26.6 | 1 | 18.4 | 1 | 43.1 | 2 |
| | 47.9 | 2 | 71.6 | 1 | 68.6 | 2 |
| | 63.4 | 1 | 90 | 1 | | |
| | 77.1 | 2 | | | | |

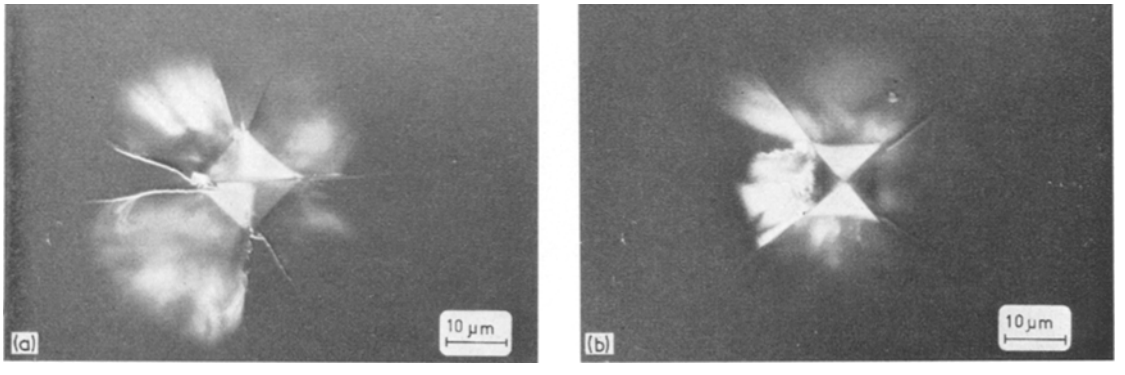


*Figure 3* (a) $Mn_{1.06}Al_{1.94}O_4$, (001) plane, indentation diagonals parallel to ⟨100⟩, 200 gf load, interference contrast. (b) Indentation diagonals parallel to ⟨110⟩.

fall beyond the stoichiometric composition $MnAl_2O_4$ (3 Al/(Al + Mn) = 2) has to be accounted for by the presence of structural vacancies, as indicated in the formula $Mn_{1-x}Al_x[Al_{2-x/3}\square_{x/3}]O_4$ (symbols in square brackets indicate Al ions and vacancies on octahedral sites). In contrast to Mg–Al spinels [27], these defects in Mn aluminates appear to promote deformability. Mn aluminates are about as hard as other aluminate spinels, as can be seen by comparison with Table IV. Aluminate and chromite spinels appear to be much harder than the ferrites, the hardness values of magnetite and hausmannite being about equal. As most hardness data are obtained on mineral specimens, and, therefore, scatter appreciably, a systematic comparison cannot be made.

To better characterize the specimens, for some selected compositions the log load versus log diagonal length relationships were established

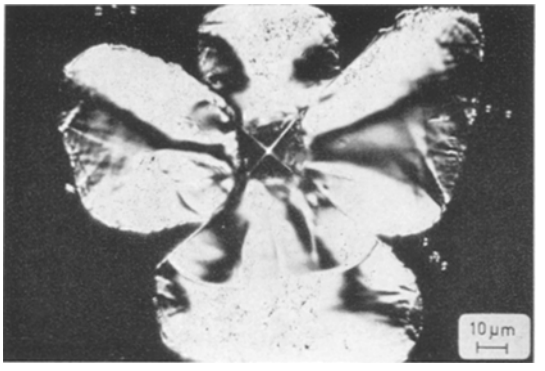


*Figure 4* Shell fractures caused by high load (500 gf), on $Mn_{1.83}Al_{1.17}O_4$, (001) plane, indentation diagonals parallel to ⟨110⟩, interference contrast (dark field).

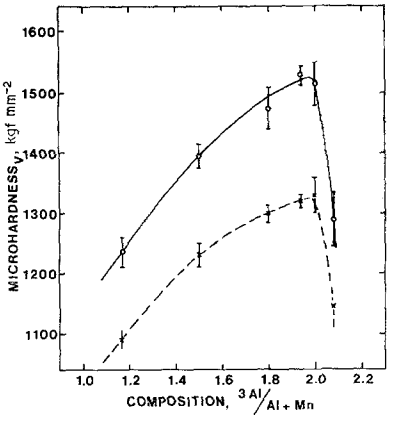


*Figure 5* Microhardness versus composition of manganese aluminates, (001) plane, indentation diagonals parallel to ⟨110⟩. ○: 50 gf load; ×: 200 gf load.

(Fig. 6a and c), which are essentially straight in the investigated region, and have a slope of 1.80 to 1.85. The predicted [2] curve has a slope of 2 at low and high load regions, in which the measured hardness is independent of applied load, and a curved transition region in between with one inflection point. Apparently the region with a slope of 2 lies at much smaller loads than

TABLE IV Vickers microhardness numbers reported for spinel-type compounds, measured when using a 100 gf load

| Name | Natural (n) or synthetic (s) | Microhardness (kgf mm$^{-2}$) | Remarks | Reference |
|---|---|---|---|---|
| Chromite ($FeCr_2O_4$) | n | 1245–1520 | | [4] |
| | n | 1035–1565 | | [28] |
| | n | 1195–1210 | | [29] |
| | n | 850–1210 | | [30] |
| | n | 1040–1170 | 200 gf load | [31] |
| Gahnite ($ZnAl_2O_4$) | n | 1490–1605 | | [4] |
| Hercynite ($FeAl_2O_4$) | n | 1380–1550 | (110) plane | [4] |
| | n | 1480–1535 | (100) plane | [4] |
| Spinel ($MgAl_2O_4$) | n | 1380–1505 | (111) plane | [4] |
| | s | 1200–1500 | dependent on composition | [27] |
| Jacobsite ($MnFe_2O_4$) | n | 840–870 | | [4] |
| | n | 725–745 | | [29] |
| Franklinite ($ZnFe_2O_4$) | n | 720–750 | (111) plane | [4] |
| | n | 765–825 | (100) plane | [4] |
| | n | 755–795 | | [28] |
| Magnetite ($Fe_3O_4$) | n | 490–660 | | [4] |
| | n | 535–695 | | [28] |
| | n | 530–600 | | [29] |
| | n | 455–495 | | [30] |
| | n | 575–630 | | [32] |
| | s | 500 | 20 gf load | [23] |
| Hausmannite ($Mn_3O_4$) | n | 495–620 | | [4] |
| | n | 540–615 | | [29] |
| | n | 385–465 | | [30] |
| | n | 495–540 | | [31] |
| | s | 425 | 50 gf load | [33] |

applied and the investigated range constitutes the transition region, but the expected curvature is not observed. Maybe the occurrence of cracks disturbs the ideal relation based purely on plastic deformation.

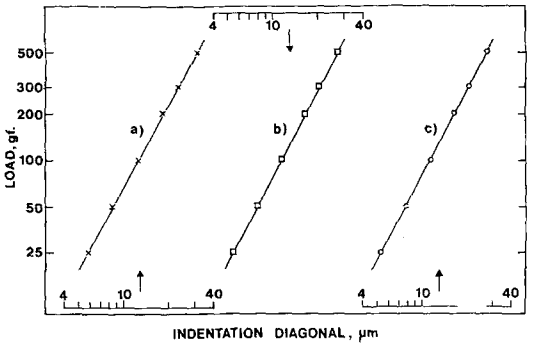


*Figure 6* Log load versus log diagonal length, on (001) plane, for: (a) $Mn_{1.83}Al_{1.17}O_4$, diagonals parallel to ⟨110⟩; (b) $Mn_{1.20}Al_{1.80}O_4$, annealed for 20 h at 920°C, diagonals parallel to ⟨100⟩; (c) $Mn_{1.06}Al_{1.94}O_4$, diagonals parallel to ⟨110⟩.

### 3.3. Effects of pre-precipitation

Hardness variations are represented as a function of annealing time at 1490°C of $Mn_{0.91}Al_{2.06}\square_{0.03}O_4$ (Fig. 7) and at 920°C of $Mn_{1.20}Al_{1.80}O_4$ (Fig. 8). At 1490°C precipitation of $\gamma$–$(Mn,Al)_2O_3$ occurs almost at the very start of annealing and the equilibrium corundum precipitate has fully developed after 1 h. At 920°C precipitation – starting at the outer surface – proceeds much more slowly and the intermediate $\gamma$ phase has not developed in the bulk of the crystal till after about 40 h. The remarkable increase in hardness at first annealing at 1490°C might be due to formation of a pre-precipitation phase as well as to precipitation of $\gamma$–$(Mn,Al)_2O_3$. Over-ageing accounts for the subsequent fall in hardness, and the accompanying shift from the hyperstoichiometric spinel to $Mn_{1.05}Al_{1.95}O_4$ (according to the phase diagram) for the remaining higher hardness. At 920°C, however, maximum hardness is reached at a point where no $\gamma$ phase is observed (unless near the outer surface where no measurements were carried out). The increase in hardness must be due to formation of a pre-precipitation phase analogous to Guinier-Preston zones in metals. At longer annealing, over-ageing occurs, finally followed by $\gamma$-phase precipitation. Its presence in the spinel accounts for the hardness being higher after prolonged annealing than that of spinel on its own. The formation of the pre-precipitation phase has no influence on the linearity of the log load versus log (diagonal length) relationship (Fig. 6b), which points to a fine dispersion of this phase.

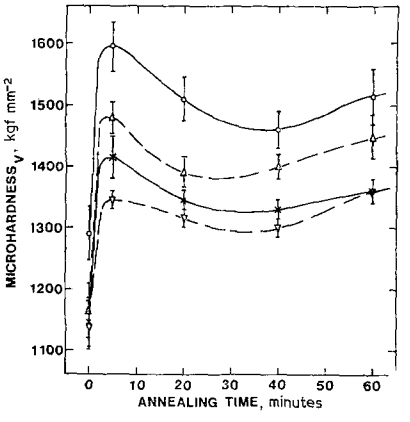


*Figure 7* Microhardness versus annealing time at 1490°C, of $Mn_{0.91}Al_{2.06}\square_{0.03}O_4$.
○: 50 gf load, (001) plane;
×: 200 gf load, (001) plane;
△: 50 gf load, near-(111) plane;
▽: 200 gf load, near-(111) plane.

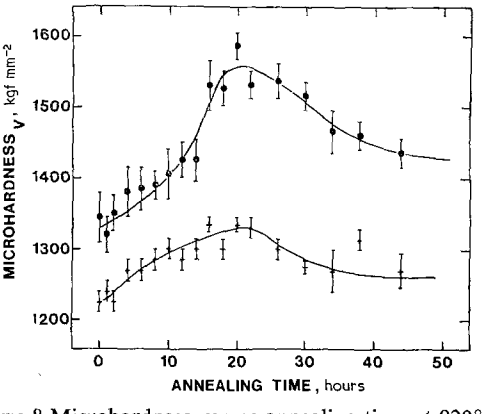


*Figure 8* Microhardness versus annealing time at 920°C, of $Mn_{1.20}Al_{1.80}O_4$, (110) plane, indentation diagonals parallel to $[1\bar{1}1]$ and $[\bar{1}12]$.
●: 50 gf load; +: 200 gf load.

The different hardness behaviour of Mn aluminates as compared with Mg aluminates can be understood from the above results. The hardness of a two-phase sample is built up by the individual hardnesses of the components and the phase boundary effect on the hardness [2]. Under

equal conditions of composition one would expect the Mn–Al spinel plus $\gamma$–$(Mn,Al)_2O_3$ to be harder than the Mg–Al spinel plus $\phi$–$MgAl_{26}O_{40}$, because the coherency of the lattices of matrix and precipitate requires no contraction of the oxygen-oxygen distances in the latter system but a 2.7% contraction in the first system [17]. As, however, the hardness of the manganese aluminates plus $\gamma$ phase is lower than that of the magnesium aluminates plus $\phi$ phase (the hardness of the aluminate spinels without precipitates being almost equal), this difference has to be attributed to a lower hardness of the $\gamma$ phase compared with the $\phi$ phase. However, the influence of precipitate distribution on the glide systems might also play its part, and then it has to be taken into account that the $\gamma$ phase precipitates on {001} habit planes [17], the $\phi$ phase on {113} habit planes [8].

## 4. Conclusions

On a (001) plane of $Mn_{1.83}Al_{1.17}O_4$ specimens the crack pattern round an indentation is independent of the relative indenter orientation and can be related to {110} glide planes. On account of height differences due to these cracks, indentation diagonals are somewhat shorter when lying along ⟨100⟩ than along ⟨110⟩, resulting in apparent hardness differences. Hardness variations on different crystallographic planes can be related to the angles of intersection of the {110} glide planes with the plane of the surface. The smaller these angles are the smaller the hardness. These results agree with the remarks of Bückle [1, 2] and Boyarskaya and Grabko [5] on hardness anisotropy, which appears to be primarily brought about by the positions and distribution of the glide planes, which are, in turn, dependent on atomic stacking.

On compounds with a higher alumina content, which are harder, other glide planes then {110} become also effective, depending on the relative orientation of the indenter. At high loads, chips (shell fractures) occur round indentations due to severe deformation.

The Vickers micro-hardness of as-grown manganese-aluminate single crystals having compositions ranging from $Mn_{1.83}Al_{1.17}O_4$ to $Mn_{0.91}Al_{2.06}\square_{0.03}O_4$ varies from 1100 to 1300 kgf mm$^{-2}$ using a 200 gf load, and from 1200 to 1500 kgf mm$^{-2}$ using a 50 gf load. A sharp decrease occurs for the hyperstoichiometric compound, probably due to structural vacancies. The relation log load versus log diagonal length is linear in the region of 25 to 500 gf load (about 4 to 40 μm diameter), having a slope of 1.80 to 1.85, depending on composition.

On the annealing of specimens, formation of a pre-precipitation phase is revealed by an increase in hardness. The log load versus log diagonal length relation is still linear, indicating a fine dispersion of this phase. On further annealing, hardness decreases by the effect of over-ageing, but remains higher in the two-phase material than in the as-grown crystal. To account for the different hardness behaviour on precipitation in Mg and Mn aluminates, the hardness of $\gamma$–$(Mn,Al)_2O_3$ is supposed to be lower than the one of $\phi$–$MgAl_{26}O_{40}$.

## Acknowledgements

The authors gratefully acknowledge the stimulating discussions with Dr Ir G. F. Bastin and Dr F. J. J. van Loo.

## References

1. H. BÜCKLE, *Met. Rev.* **4** (1959) 49.
2. *Idem*, "L'essai de microdureté et ses applications". (Publications Scientifiques et Techniques du Ministère de l'Air, Paris 1960) (German Translation: Berliner Union, Stuttgart, 1965).
3. YU. S. BOYARSKAYA, D. Z. GRABKO and J. J. MELENT'EV, *Izv. Akad. Nauk. Mold. S.S.R., Ser. Fiz. Tekh. Mat. Nauk.* (1971) 30.
4. B. B. YOUNG and A. P. MILLMAN, *Inst. Mining Met., Trans.* **73** (1963/4) 437.
5. YU. S. BOYARSKAYA and D. Z. GRABKO, *Krist. Tech.* **8** (1973) 1367.
6. H. WINCHELL, *Amer. Mineral.* **30** (1945) 583.
7. T. ITO, *J. Amer. Ceram. Soc.* **54** (1971) 24.
8. H. SAALFELD and H. JAGODZINSKI, *Z. Kristallogr.* **109** (1957) 87.
9. J. G. GRABMAIER and H. R. FALCKENBERG, *J. Amer. Ceram. Soc.* **52** (1969) 648.
10. W. F. EPPLER, *Z. angew. Mineral.* **4** (1943) 345.
11. A. MANGIN and H. FORESTIER, *Compt. Rend. Acad. Sci.* **242** (1956) 1893.
12. D. VIECHNICKI, F. SCHMID and J. W. MCCAULEY, *J. Appl. Phys.* **43** (1972) 4508.
13. A.-M. LEJUS and R. COLLONGUES, *Compt. Rend. Acad. Sci.* **251** (1960) 959.
14. A.-M. LEJUS, *Rev. Hautes Temp. Réfract.* **1** (1964) 53.
15. V. S. STUBICAN, C. GRESKOVICH and H. A. MCKINSTRY, *J. Amer. Ceram. Soc.* **52** (1969) 174.
16. E. H. L. J. DEKKER and G. D. RIECK, *Rev. Int. Hautes Temp. Refract.* **11** (1974) [3] to be published.
17. E. H. L. J. DEKKER and G. D. RIECK, *J. Cryst. Growth.* **23** (1974) 143.
18. A. S. KEH, J. C. M. LI and Y. T. CHOU, *Acta Met.* **7** (1959) 694.

19. M. H. LEWIS, *Phil. Mag.* **17** (1968) 481.
20. K. C. RADFORD and C. W. A. NEWEY, *Proc. Brit. Ceram. Soc.* **9** (1967) 131.
21. C. W. A. NEWEY and K. C. RADFORD, in "Anisotropy in single-crystal refractory compounds", Proceedings of the International Symposium, Dayton 1967 (edited by F. W. Vahldiek and S. A. Mersol) (Plenum Press, New York, 1968) Vol. 2, p. 321.
22. N. DOUKHAN, R. DUCLOS and B. ESCAIG, *J. Phys. (Paris)* **34** (1973) C9: 379.
23. P. CHARPENTIER, P. RABBE and J. MANENC, *Mater. Res. Bull.* **3** (1968) 69.
24. J. H. WESTBROOK and P. J. JORGENSEN, *Trans. Met. Soc. AIME* **233** (1965) 425.
25. *Idem*, in "Anisotropy in single-crystal refractory compounds", Proceedings of the International Symposium, Dayton 1967 (edited by F. W. Vahldiek and S. A. Mersol) (Plenum Press, New York, 1968) Vol. 2, p. 353.
26. H. TERTSCH, *Neues Jahrb. Mineral., Monatsh.* (1951) 73.
27. J. H. WESTBROOK, *Rev. Hautes Temp. Réfract.* **3** (1966) 47.
28. S. I. LEBEDEVA, *Tr. Inst. Mineralog., Geokhim. i. Kristallokhim. Redkikh Elementov, Akad. Nauk. SSSR* (1961) 89.
29. S. H. U. BOWIE and K. TAYLOR, *Mining Mag.* **99** (1958) 265, 337.
30. J. SIEBEL, *Metall. Erz.* **40** (1943) 169.
31. G. TOUBEAU, *Bull. Soc. Belge Géol.* **71** (1962) 242.
32. F. ZÁBRANSKY and J. DRABANT, *Geol. Zb. (Bratislava)* **21** (1970) 99.
33. G. C. WOOD and T. HODGKIESS, *Werkst. Korros.* **23** (1972) 766.

Received 22 May and accepted 13 June 1974